Soft Matter

Cite this: *Soft Matter*, 2012, **8**, 7138

www.rsc.org/softmatter

PAPER

Surface wrinkling in liquid crystal elastomers†

Aditya Agrawal,[a] Paul Luchette,[b] Peter Palffy-Muhoray,[b] Sibani Lisa Biswal,[a] Walter G. Chapman[a] and Rafael Verduzco*[a]

Received 29th March 2012, Accepted 16th May 2012
DOI: 10.1039/c2sm25734c

Structured surfaces give rise to novel and potentially useful properties such as controllable wettability and structural colour. Here, we demonstrate structured surfaces *via* reversible surface wrinkling in liquid crystal elastomers (LCEs). A thin polymer film deposited on top of a shape-responsive LCE exhibits a reversible, periodic surface wrinkling pattern in response to temperature changes. The orientation of the wrinkles depends on the orientation of the nematic director and the temperature at which the bilayer is prepared, and the wrinkles can be re-oriented in a single sample by heating or cooling the sample above or below the preparation temperature. We show that this bilayer system can be used to measure the modulus of nanoscale thin poly(styrene) films deposited on the LCE. Additionally, when a micron-thick polymer film is deposited on top of an LCE, the bilayer exhibits reversible curling with temperature. This system provides a simple method for measuring the mechanical properties of thin polymer films without the need for clamping and mechanical stretching and provides a new approach to generate reversible, microstructured surfaces.

Introduction

Periodic surface structures lead to novel properties and functionality. Some well-known examples from nature include structural colors in hummingbird feathers[1] and butterfly wings[2] as well as the self-cleaning properties of the lotus leaf.[3] Surface wrinkles have been used for over two decades to measure the forces generated by cells moving across a surface,[4–6] and more recent work has taken advantage of mechanically induced surface wrinkling patterns to characterize the mechanical properties of nanoscale thin films.[7,8] Additionally, superhydrophobic surfaces[9] and surfaces with reversible wettability[10] can be fabricated by controlling the surface topography.

Here, we report surface wrinkling in liquid crystal elastomers (LCEs), which exhibit large, spontaneous shape changes in response to temperature. LCEs are rubbery polymeric networks with long-range orientational and/or positional order.[11,12] Cross-linking of a poly(methylhydrosiloxane) (PHMS) polymer functionalized with liquid crystal molecules, also known as mesogens, results in a rubbery network with anisotropic mechanical properties and stimuli-responsive behaviour. In particular, LCEs can change shape reversibly in response to light,[13–15] temperature,[16,17] and electric fields.[18–20] Shape-changes in monodomain LCEs, which have a uniformly aligned liquid crystal (LC) director, can range from 10% to 400% of the initial LCE size.

We envisioned that LCEs could be used to generate reversible, periodic, and oriented surface patterns in response to modest temperature changes. Surface wrinkles induced by temperature changes have been reported using a poly(dimethylsiloxane) (PDMS)[21] and shape-memory polymers,[22] but LCEs offer fully reversible shape-changes. Other approaches for inducing surface wrinkling in elastomers include mechanical strain[7,8] and osmotic stresses from solvent swelling.[23–26] Surface wrinkles can also be produced in thin films of liquid crystal polymer without the use of an elastomer.[27]

Herein, we show that LCEs provide a reliable substrate for generating reversible surface wrinkles. Surface wrinkling can be induced in LCE–poly(styrene) (PS) bilayers by both increasing and decreasing temperature, and wrinkles can be re-oriented in a single sample by heating or cooling above the temperature at which the bilayer was prepared. Furthermore, surface wrinkles in LCEs can be used to measure the moduli of nanoscale thin PS films, down to a thickness of 30 nm. Finally, deposition of a micrometer-thick PS film on top of the LCE gives an elastomer which reversibly curls over a small (30–50 °C) temperature range.

Result and discussion

Bilayers composed of a thin polymeric film on top of a thick and deformable PDMS substrate exhibit surface wrinkling patterns in response to mechanical deformation. The patterns result from the in-plane compressive strain at the substrate–film interface and represent a compromise between the energy required to bend the stiff film and deform the PDMS substrate.[7,28,29] We envisioned that spontaneous shape-changes in LCEs in response to

[a]*Chemical and Biomolecular Engineering, Rice University, Houston, TX, 77005, USA. E-mail: rafaelv@rice.edu*
[b]*Liquid Crystal Institute, Kent State University, Kent, OH 44240, USA*
† Electronic supplementary information (ESI) available. See DOI: 10.1039/c2sm25734c

external stimuli (heat) could be used to generate the in-plane compressible strain needed to induce wrinkling instability. To test this, uniformly aligned, side-chain nematic LCEs were prepared by the two-step crosslinking method.[30] Briefly, the hydrosilylation reaction of a vinyl terminated mesogen and a diacrylate crosslinker (10 mol%) with PHMS results in a lightly crosslinked LC network with uniform alignment due to strain imposed during crosslinking (Fig. 1). Alignment is confirmed by polarized optical microscopy and by the reversible shape-change of the LCE with temperature (Fig. 2). Monodomain LCEs spontaneously change shape as a function of temperature due to the temperature dependent order parameter of the LC mesogens, and the shape change is fully reversible on both heating and cooling the sample. Next, nanoscale PS films were prepared by spin-casting a 0.25–3 wt% PS solution (M_w = 271 kg mol^{-1}, polydispersity = 1.02, Polymer Standards Service-USA Inc) onto a silicon substrate cleaned by UV-ozone treatment. To transfer the PS film to the LCE substrate, the LCE was gently placed on top of the PS film, immersed in water at a fixed temperature for 10 hours, and then peeled off and dried under vacuum. This method can be used to prepare LCE–PS bilayers with different PS film thicknesses and at different preparation temperatures.

To test whether surface wrinkling could be induced with temperature changes in LCE bilayers, we prepared two PS–LCE bilayer samples, both with a 30 nm PS film and a 0.36 mm thick LCE. The first sample was prepared by film transfer at 30 °C and the second at 60 °C. Surface wrinkling in both of these samples was monitored using optical microscopy equipped with a home-built heat stage. As shown in Fig. 3, the sample prepared at 30 °C is uniform at room temperature but exhibits surface wrinkling when the temperature is increased to 40 °C. As the temperature increases, the LC order parameter decreases and the LCE spontaneously deforms, with contraction along the director (and dilation in the perpendicular directions) resulting in surface wrinkles above a critical strain (approximately 5%, achieved at 40 °C). Conversely, for the sample prepared at 60 °C, surface wrinkles oriented parallel to the nematic director appear upon cooling the sample. The LC order parameter increases as the temperature is decreased, resulting in a spontaneous elongational strain in the direction parallel to the global nematic director (and compressive stress normal to the director). For both cases, the wavelength of the surface wrinkles is independent of temperature above the critical strain.

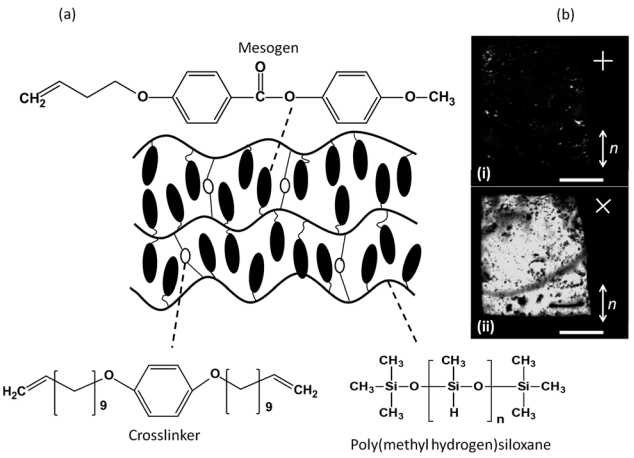

Fig. 1 (a) Schematic and structure of polysiloxane based side-chain LCE. (b) Optical microscopy images of LCE between crossed polarizers with the nematic director *n* oriented at (i) 0 °C and (ii) 45 °C with respect to crossed polarizers. Scale bars represent 50 μm.

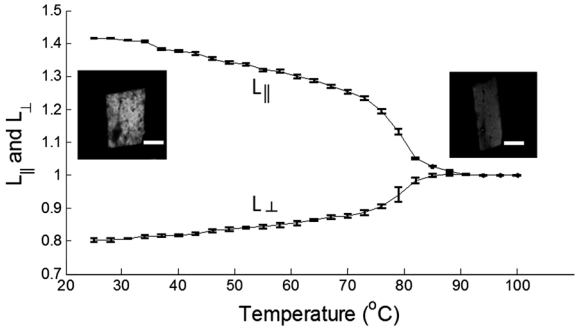

Fig. 2 Shape change of LCE (10% crosslinking density) with temperature. $L_{\parallel}$: normalized LCE dimension parallel to director; $L_{\perp}$: normalized LCE dimension perpendicular to director. Normalization was done w.r.t. corresponding isotropic lengths. The inset images show the shape change monitored at 35 and 90 °C under crossed polarizers. Scale bars represent 80 μm.

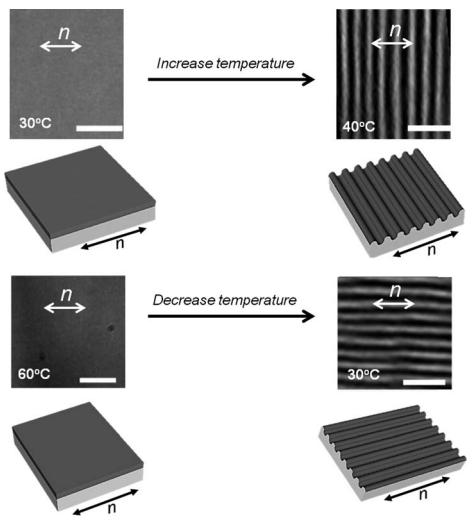

Fig. 3 Optical microscopy images of the top surface of LCE bilayer samples prepared at (a) 30 °C and at (b) 60 °C along with schematic images of the surface wrinkling instability. *n* represents the orientation of LCE nematic director, and all scale bars represent 10 μm.

While previous work has demonstrated temperature-induced surface wrinkling,[21,22] LCE bilayers uniquely enable the reversible reorientation of wrinkles with temperature in a single sample. As shown in Fig. 4a, an LCE–PS bilayer (35 nm PS and 0.36 mm LCE) prepared at 50 °C is uniform at 50 °C but exhibits surface wrinkles parallel to the nematic director if the sample is cooled below the preparation temperature. Conversely, if the sample is heated above the preparation temperature (to 60 °C) surface wrinkles appears oriented perpendicular to the nematic director. This response is fully reversible with temperature.

While relatively small temperature changes (20–30 °C) below the glass-transition temperature T_g of the PS film give reversible surface wrinkling patterns, larger temperature changes over

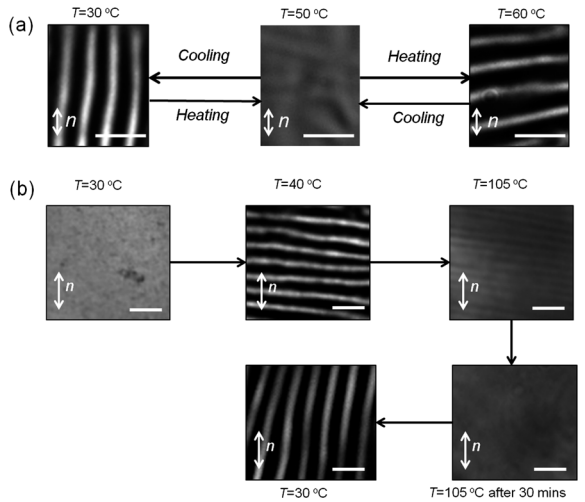

Fig. 4 Optical microscopy images of the top surface of a PS–LCE bilayer (a) prepared at 50 °C (scale bars: 5 μm) and (b) prepared at 30 °C (scale bars: 10 μm). In (a), wrinkles are re-oriented in a single sample by heating or cooling past the preparation temperature. In (b), wrinkles are reoriented by heating to the T_g of PS, annealing the sample, and then cooling. *n* represents the orientation of LCE nematic director.

a range that exceeds the T_g of the PS film can also be used to erase and re-orient surface wrinkles. To demonstrate this, a 50 nm PS thin film was transferred onto the LCE substrate at 30 °C and subsequently heated to the T_g (~105 °C) of the PS film (Fig. 4b). Surface wrinkles oriented perpendicular to the nematic director appear at temperatures below the T_g, but upon annealing the sample near the T_g of PS, surface wrinkles are 'erased' due to viscoelastic flow of the PS film. The surface becomes uniform after annealing for approximately 30 minutes, and on subsequent cooling surface wrinkles reappear oriented parallel to the nematic director. One drawback of this technique is that large temperature variations are associated with large strains that can cause cracking or delamination of the PS films (see examples in ESI†). Similar phenomena have been reported in previous studies.[31–35] The formation of cracks in the top PS film makes the LCE based wrinkling instability reversible only for small strain values (<5%), but the modulus of the top polymer film and the nematic-to-isotropic transition temperature of the LCE can be tuned to target a desired temperature range.

Surface wrinkles in bilayer samples are a type of Euler buckling instability[36] where the stiff, thin film (PS in the present study) is in contact with a softer and thicker substrate; compressive stress leads to more favourable short wavelength displacements in-comparison to simple bowing. The wavelength of the surface wrinkles can be quantitatively described using the Euler–Bernoulli beam-bending equation[7,37,38] with the assumption that the polymer film is significantly thinner than the LCE substrate and has a substantially greater modulus. As shown in eqn (1), the wavelength λ of the surface wrinkling patterns depends on the film thickness h, the film plane-strain modulus $\bar{E}_f = E_f/(1-\nu_f^2)$, where E_f and ν_f are the Young's modulus and Poisson's ratio for the film, respectively, and the substrate plane-strain modulus $\bar{E}_s = E_s/(1-\nu_s^2)$, where E_s and ν_s are the Young's modulus and Poisson's ratio of substrate, respectively.

$$\lambda = 2\pi h\left(\frac{\bar{E}_f}{3\bar{E}_s}\right)^{1/3} \quad (1)$$

The relationship in eqn (1) forms the basis of the technique known as strain-induced elastic buckling instability for mechanical measurements (SIEBIMM)[8] and enables calculation of the thin film modulus *via* measurement of the wavelength of surface wrinkles and the modulus of the deformable substrate. This method has been used to characterize the properties of a variety of materials, including metal films,[40] polymer brushes,[41,42] polymer nanocomposites,[43] carbon nanotubes,[44] among others.[7] Here, we will apply SIEBIMM to measure the modulus of the nanoscale PS films and to test whether the relationship between the surface wrinkle wavelength and film modulus follows eqn (1). The elastic modulus of the LCE substrate was measured with a dynamic mechanical analyzer (DMA-Q800) and found to be 0.24 MPa. Using the same LCE sample, we tested PS film thicknesses ranging in thickness from 30 nm up to 400 nm (Fig. 5). Samples were prepared at room temperature and heated to 40 °C to create surface wrinkles, and the wavelength of surface wrinkles was measured with an optical microscope. As shown in Fig. 5a and b, the wavelength increases linearly with PS film thickness and varies from 2 μm up to 40 μm over this PS film thickness range. By applying eqn (1), we find that for film thicknesses greater than 100 nm, the measured modulus is in good quantitative agreement with the bulk PS modulus of 3.5 GPa.[8,45] At film thicknesses below 50 nm, we observe a drop in the film modulus, similar to what has been previously observed in SIEBIMM measurements.[39,46] These data indicate that LCEs are reliable substrates for measurement of polymer moduli *via* SIEBIMM without the need for clamping the sample.

Above a critical thickness of the PS film (for 0.36 mm thick LCE), surface wrinkling is no longer favoured. Instead, due to

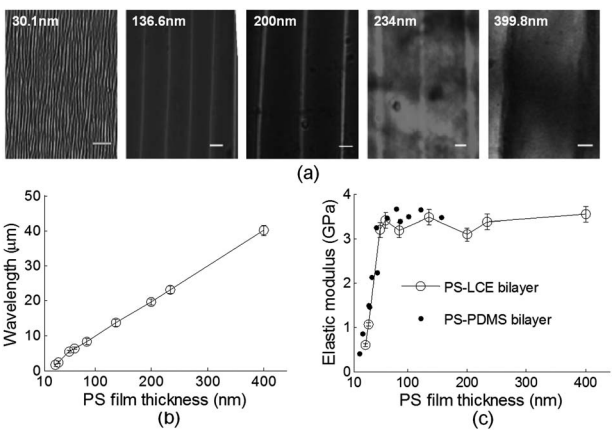

Fig. 5 (a) Optical microscopy images showing wrinkling patterns of PS–LCE bilayers with varying PS film thicknesses, measured by spectroscopic ellipsometry and indicated by the number at the top of each image. Dependence of wrinkling wavelength (b) and elastic modulus (c) on the PS film thickness. The data points and error bars were evaluated by repeating each measurement six times. Scale bars represent 10 μm for all images shown. The experimental data for PS–PDMS bilayers shown were reported by Vogt *et al.*[39] and were acquired by mechanically straining the bilayer sample.

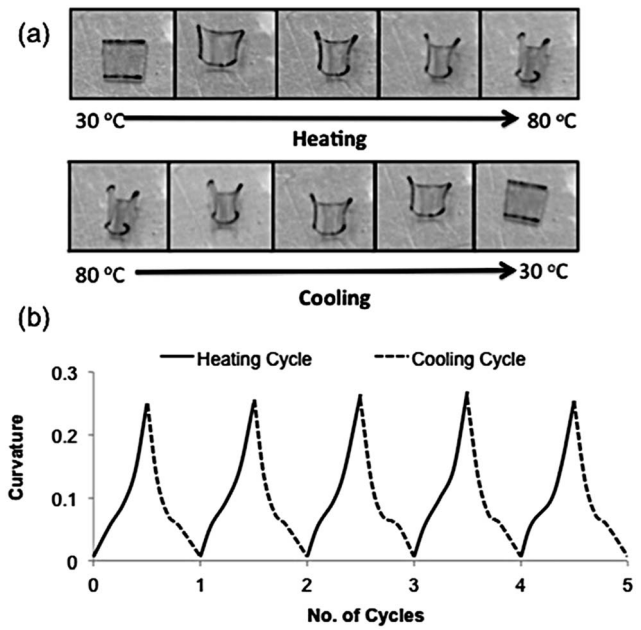

Fig. 6 (a) PS–LCE which reversibly curls with temperature and (b) curvature of PS–LCE bilayer as a function of number of heating and cooling cycles. PS film and LCE substrate were 986 nm and 0.36 mm in thickness, respectively. Curvature was measured by taking images of the LCE sample during heating and cooling cycles and processing the images using ImageJ 1.440.

the elongational anisotropy of the PS and LCE films, PS–LCE bilayers exhibit reversible curling. This was observed for a bilayer sample prepared at room temperature with a 986 nm thick PS film and 0.36 mm thick LCE. While initially flat at room temperature, the bilayer reversibly curls over a temperature range of 30–80 °C, near the nematic-to-isotropic transition temperature (T_{NI}) of the LCE (see Fig. 6 and video in ESI†). The LCE curling phenomenon is found to be very reversible (Fig. 6b), with only slight hysteresis is observed after subjecting the sample to several heating and cooling cycles. This response analogous to the bending and twisting of elastomers by non-homogeneous swelling[47] and the reversible curling in metallic bilayer strips,[48–52] where the curvature of bilayer is proportional to the difference in elongation of the two layers. An advantage of the PS–LCE bilayer system is the large strains that are achieved over a temperature range of approximately 30–50 °C. The performance is comparable to those demonstrated in dielectric elastomer actuators (strains up to 300% have been reported by applying an electric field of 420 MV m^{-1})[53,54] but can be achieved with temperature changes instead of external voltages.

Experimental

Synthesis of LCE

The LCEs were synthesized by the previously reported two-step crosslinking method.[19] Briefly, LC (mesogen) monomer, crosslinker, and PHMS (Fig. 1) are dissolved in toluene along with platinum catalyst dichloro(1,5-cyclooctadiene)platinum(II). First, partial crosslinking is achieved by heating the reaction mixture for several hours. In a second step, the partially crosslinked elastomer is stretched by applying a load and then annealed at room temperature for several days. This results in uniform orientation of director along the stretching direction. For this study, LCEs with 10% crosslinking density were used.

Conclusions

In summary, we have demonstrated that LCEs can be used to generate reversible, periodic surface patterns. Surface wrinkles spontaneously develop with temperature changes due to the temperature dependent shape of the LCE substrate, and the orientation of the surface wrinkles is either parallel or perpendicular to the nematic director, depending on the sample preparation conditions and direction of temperature change. Surface wrinkles can be reoriented in a single sample by heating and cooling beyond the sample preparation temperature. LCEs can be used to accurately measure the moduli of nanoscale polymer films *via* SIEBIMM, and above a critical thickness ratio of PS film to LCE substrate the PS–LCE bilayer exhibits reversible curling with temperature. In addition to measuring thin-film moduli by SIEBIMM, polymer–LCE bilayers are potentially useful for nanoparticle assembly and as polymeric actuators.

Acknowledgements

This project was supported in part by the IBB Hamill Innovation Grant and Louis and Peaches Owen. A. Agrawal and W. G. Chapman acknowledge financial support of the Robert A. Welch Foundation (Grant no. C-1241) and NSF CBET-0756166.

Notes and references

1 C. H. Greenewalt, W. Brandt and D. D. Friel, *J. Opt. Soc. Am.*, 1960, **50**, 1005.
2 P. Vukusic, J. R. Sambles and C. R. Lawrence, *Nature*, 2000, **404**, 457.
3 W. Barthlott and C. Neinhuis, *Planta*, 1997, **202**, 1–8.
4 E. Cerda and L. Mahadevan, *Phys. Rev. Lett.*, 2003, **90**, 074302.
5 A. Harris, P. Wild and D. Stopak, *Science*, 1980, **208**, 177–179.
6 K. Burton, J. H. Park and D. L. Taylor, *Mol. Biol. Cell*, 1999, **10**, 3745–3769.
7 J. Y. Chung, A. J. Nolte and C. M. Stafford, *Adv. Mater.*, 2011, **23**, 349–368.
8 C. M. Stafford, C. Harrison, K. L. Beers, A. Karim, E. J. Amis, M. R. VanLandingham, H.-C. Kim, W. Volksen, R. D. Miller and E. E. Simonyi, *Nat. Mater.*, 2004, **3**, 545–550.
9 D. Wu, Q.-D. Chen, H. Xia, J. Jiao, B.-B. Xu, X.-F. Lin, Y. Xu and H.-B. Sun, *Soft Matter*, 2010, **6**, 263–267.
10 T. Sun, G. Wang, L. Feng, B. Liu, Y. Ma, L. Jiang and D. Zhu, *Angew. Chem.*, 2004, **116**, 361–364.
11 M. Warner and E. M. Terentjev, *Liquid Crystal Elastomers*, Oxford University Press, 2003.
12 K. Urayama, *Macromolecules*, 2007, **40**, 2277–2288.
13 M. Yamada, M. Kondo, R. Miyasato, Y. Naka, J.-i. Mamiya, M. Kinoshita, A. Shishido, Y. Yu, C. J. Barrett and T. Ikeda, *J. Mater. Chem.*, 2009, **19**, 60–62.
14 H. Finkelmann, E. Nishikawa, G. G. Pereira and M. Warner, *Phys. Rev. Lett.*, 2001, **87**, 015501.
15 M. Camacho-Lopez, H. Finkelmann, P. Palffy-Muhoray and M. Shelley, *Nat. Mater.*, 2004, **3**, 307–310.
16 C. Ohm, M. Brehmer and R. Zentel, *Adv. Mater.*, 2010, **22**, 3366–3387.
17 Y. Sawa, K. Urayama, T. Takigawa, A. DeSimone and L. Teresi, *Macromolecules*, 2010, **43**, 4362–4369.
18 A. Sánchez-Ferrer, T. Fischl, M. Stubenrauch, H. Wurmus, M. Hoffmann and H. Finkelmann, *Macromol. Chem. Phys.*, 2009, **210**, 1671–1677.

19 M. D. Kempe, N. R. Scruggs, R. Verduzco, J. Lal and J. A. Kornfield, *Nat. Mater.*, 2004, **3**, 177–182.
20 A. Fukunaga, K. Urayama, T. Takigawa, A. DeSimone and L. Teresi, *Macromolecules*, 2008, **41**, 9389–9396.
21 N. Bowden, W. T. S. Huck, K. E. Paul and G. M. Whitesides, *Appl. Phys. Lett.*, 1999, **75**, 2557–2559.
22 T. Xie, X. Xiao, J. Li and R. Wang, *Adv. Mater.*, 2010, **22**, 4390–4394.
23 M. Guvendiren, S. Yang and J. A. Burdick, *Adv. Funct. Mater.*, 2009, **19**, 3038–3045.
24 E. P. Chan, E. J. Smith, R. C. Hayward and A. J. Crosby, *Adv. Mater.*, 2008, **20**, 711–716.
25 H. S. Kim and A. J. Crosby, *Adv. Mater.*, 2011, **23**, 4188–4192.
26 J. Y. Chung, A. J. Nolte and C. M. Stafford, *Adv. Mater.*, 2009, **21**, 1358–1362.
27 S. H. Kang, J.-H. Na, S. N. Moon, W. I. Lee, P. J. Yoo and S.-D. Lee, *Langmuir*, 2012, **28**, 3576–3582.
28 R. Huang, *J. Mech. Phys. Solids*, 2005, **53**, 63.
29 A. L. Volynskii, S. Bazhenov, O. V. Lebedeva and N. F. Bakeev, *J. Mater. Sci.*, 2000, **35**, 547.
30 J. Kupfer and H. Finkelmann, *Makromol. Chem., Rapid Commun.*, 1991, **12**, 717–726.
31 A. L. Volynskii, S. Bazhenov, O. V. Lebedeva and N. F. Bakeev, *J. Mater. Sci.*, 2000, **35**, 547–554.
32 S. L. Bazhenov, I. V. Chernov, A. L. Volynskii and N. F. Bakeev, *Dokl. Akad. Nauk*, 1997, **356**, 199–201.
33 Y. Leterrier, L. Boogh, J. Andersons and J. A. E. Manson, *J. Polym. Sci., Part B: Polym. Phys.*, 1997, **35**, 1449–1461.
34 N. M. Martyak, J. E. McCaskie, B. Voos and W. Plieth, *J. Mater. Sci.*, 1997, **32**, 6069–6073.
35 A. L. Volynskii, S. L. Bazhenov, O. V. Lebedeva, A. N. Ozerin and N. F. Bakeev, *Vysokomol. Soedin., Ser. A Ser. B*, 1997, **39**, 1827–1832.
36 L. D. Landau and E. M. Lifshits, *Theory of Elasticity*, Moscow, 3rd edn, 1965.
37 S. P. Timoshenko, *History of Strength of Materials with a Brief Account of the History of Theory of Elasticity and Theory of Structures*, McGraw-Hill Book Co., 1953.
38 M. A. Biot, *ASME J. Appl. Mech. A*, 1937, **59**, 1–7.
39 J. M. Torres, C. M. Stafford and B. D. Vogt, *Polymer*, 2010, **51**, 4211–4217.
40 N. Bowden, S. Brittain, A. G. Evans, J. W. Hutchinson and G. M. Whitesides, *Nature*, 1998, **393**, 146–149.
41 H. Huang, J. Y. Chung, A. J. Nolte and C. M. Stafford, *Chem. Mater.*, 2007, **19**, 6555–6560.
42 M. Wang, J. E. Comrie, Y. Bai, X. He, S. Guo and W. T. S. Huck, *Adv. Funct. Mater.*, 2009, **19**, 2236–2243.
43 J.-Y. Lee, K. E. Su, E. P. Chan, Q. Zhang, T. Emrick and A. J. Crosby, *Macromolecules*, 2007, **40**, 7755–7757.
44 D.-Y. Khang, J. Xiao, C. Kocabas, S. MacLaren, T. Banks, H. Jiang, Y. Y. Huang and J. A. Rogers, *Nano Lett.*, 2008, **8**, 124–130.
45 K. Miyake, N. Satomi and S. Sasaki, *Appl. Phys. Lett.*, 2006, **89**, 031925/1–031925/3.
46 K. F. Mansfield and D. N. Theodorou, *Macromolecules*, 1991, **24**, 6283–6294.
47 D. P. Holmes, M. Roche, T. Sinha and H. A. Stone, *Soft Matter*, 2011, **7**, 5188–5193.
48 S. Timoshenko, *J. Opt. Soc. Am. Rev. Sci. Instrum.*, 1925, **11**, 233–255.
49 G. G. Stoney, *Proc. R. Soc. London, Ser. A*, 1909, **82**, 172.
50 B. Simpson, G. Nunnery, R. Tannenbaum and K. Kalaitzidou, *J. Mater. Chem.*, 2010, **20**, 3496–3501.
51 V. Luchnikov, O. Sydorenko and M. Stamm, *Adv. Mater.*, 2005, **17**, 1177–1182.
52 K. Kalaitzidou and A. J. Crosby, *Appl. Phys. Lett.*, 2008, **93**, 041910/1–041910/3.
53 R. Shankar, T. K. Ghosh and R. J. Spontak, *Soft Matter*, 2007, **3**, 1116–1129.
54 H. Soon Mok, Y. Wei, P. Qibing, P. Ron and S. Scott, *Smart Mater. Struct.*, 2007, **16**, S280.

Addition and correction

Note from RSC Publishing

This article was originally published with incorrect page numbers. This is the corrected, final version.

The Royal Society of Chemistry apologises for these errors and any consequent inconvenience to authors and readers.